RoboWrangler: Toward Rope-based Grasping for Mobile Manipulation

Christian Friedrich[1], Mario Gomez-Andreu[1], Gabriel Métois[1], Fan Shi[1,2], Marco Hutter[1], and Robert Baines[1]

***Abstract*— Rope is a versatile tool that has been used throughout history for numerous applications, thanks to its ability to conform to different shapes and manipulate objects of various length scales, textures, and masses. Rope could therefore be a viable tool for expanding the functionality of robots operating in human environments. In this paper, we present a rope-based manipulator that can be equipped to robots' end-effectors and used to ensnare objects and interact with environmental infrastructure. The manipulator operates by accelerating a loop of rope into a free-floating lasso-like shape whose size can be adjusted on demand. We study key variables that govern the loop shape, assess the rope manipulator's ability to grasp a variety objects, propose a physical model for simulation of rope manipulation, and demonstrate the concept's application potential when attached to a quadrupedal robot. We find that the manipulator enables wrangling of diverse objects and can be used to functionalize the existing appendages of a teleoperated quadruped robot, empowering the robot to pick up tools, open doors, and engage in manipulation of large objects. Overall, this work provides a foundation for creating and controlling a new class of rope-based robotic manipulators, serving as a testament to how passive mechanical features may be exploited to enrich manipulation capabilities.**

I. Introduction

As robots enter human environments and perform increasingly difficult tasks, they must interact with myriad objects and infrastructural features. Many manipulation systems have been proposed throughout the years to tackle the challenges of interaction in unstructured environments, ranging from rigid joint-linkage anthropomorphic hands to under-actuated soft robotic grippers and octopus-inspired continua [1], [2]. While highly-articulated designs can suffer from mechanical and control complexity (for example, many robotic hands in use today require multiple actuators per finger to coordinate 14 or more degrees of freedom (DOF) [3], [4]), under-actuated grippers, such as soft pneumatic grippers or tendon-driven structures, offer simplified mechanical designs and lower control effort [5], [6]. Moreover, the passive conformation of soft materials can be leveraged to manipulate objects that are otherwise challenging for traditional rigid grippers [7].

Although there is a wealth of existing manipulation systems, there are scant solutions that can adapt to handle objects across a range of scales (e.g. cm to m), masses (e.g. g to kg), and textural qualities [1]—all while remaining straightforward to control and integrate with robotic platforms. Generalizability, simplicity, and integrability are crucial criteria for equipping the next-generation of robots with the skills necessary to engage in tasks in unstructured human environments.

[1]ETH Zurich, Robotics Systems Lab; Leonhardstrasse 21, 8092 Zurich, Switzerland. [2]National University of Singapore. Contact: rbaines@ethz.ch

Fig. 1. RoboWrangler grasping a screwdriver from a toolbox. Leveraging the passive deformation of rope enables the robot to grasp various objects of different sizes, textures, and masses, as well as interact with infrastructural features in its environment.

Enter rope: Humans have used rope throughout history for numerous purposes, including wrangling animals, sailing, and lifting heavy objects during construction [8]. Due to its high tensile stiffness and relatively low bending stiffness, rope can conform to different shapes, exert strong forces, and grip strongly onto surfaces (e.g. through the capstan effect). These versatile mechanical qualities suggest that rope has promise as a technology in a robotic manipulator. However, reliably prescribing the shape of rope, modelling how it interacts with objects, and controlling how objects are subsequently manipulated with the rope are major challenges.

Previous work has striven to manipulate rope with a robotic hand using vision-based techniques, but does not use rope itself as a manipulator [9], [10]. Other efforts to recreate wrangling techniques used by humans, such as the traditional lasso and are limited to trick roping without object interaction [11]. In lieu of more sophisticated methods implemented by human handlers to render rope loops, robots could possibly adopt a technology akin to toy "string shooters" [12], [13], [14], [15].

In a string shooter, a string connected end-to-end is constrained to go through a fixed point where proximate rotating surfaces impart momentum on the string to accelerate it to a takeoff velocity (ToV). At ToV, the string transitions from a slack state to a continuously rotating, air-lifted state with an approximately ellipsoid shape (Fig. 2a). This ellipsoid could, in principle, be used to grasp objects, serving as the basis for a new class of rope-based manipulators.

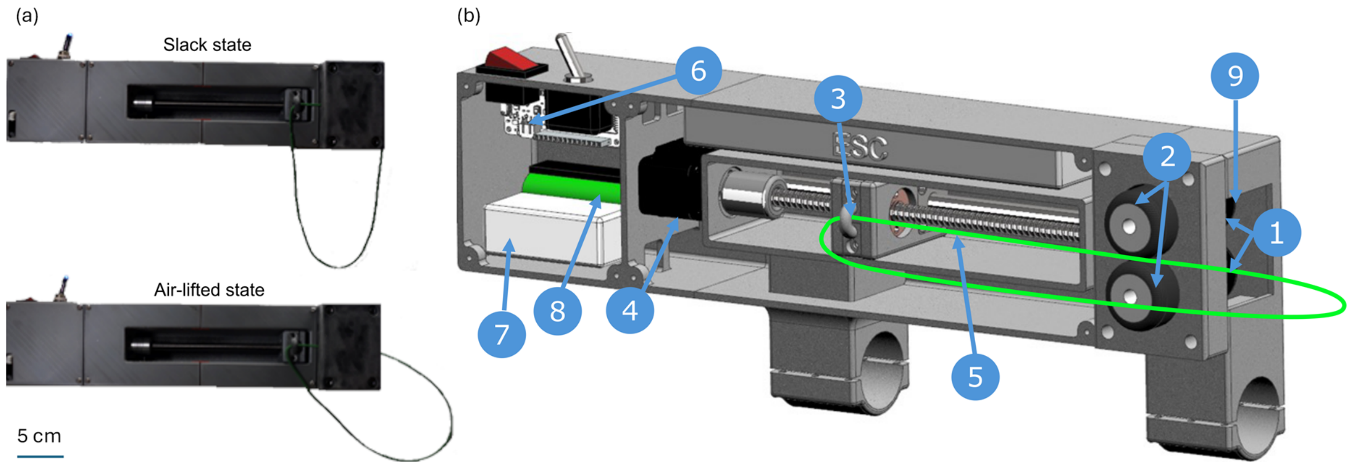

Fig. 2. An independently powered and controlled rope-based manipulator. (a) Images of manipulator with rope in slack and air-lifted (after being sped to a takeoff velocity) states. (b) 3D model of the manipulator with select electronics covers removed for clarity, highlighting (1) BLDC motors, (2) rubber wheels, (3) rope guide, (4) servo motor that controls the retraction degree-of-freedom, (5) spindle that the rope guide travels along, (6) Arduino MKR 1010 that controls all actuation functionality, (7) 12V battery, (8) 3.7V battery, and (9) magnetic encoder. The rope routing path is depicted by the green curve.

In this paper, we strive to tackle challenges of manipulating objects of different size scales, masses, and textures through the following contributions:

- Introducing a rope-based manipulator module, inspired by the physics of a string shooter, to reliably control the shape of a rope and interact with the environment.
- Developing a computational model for the rope manipulator and incorporating it into a physics-based simulation in IsaacGym.
- Integrating the rope manipulator into a quadrupedal robot, creating a "RoboWrangler," and demonstrating its utility for mobile manipulation tasks (Fig. 1).

By exploiting the physical intelligence afforded by rope [16], we circumvent the need for precise control of many individual degrees of freedom and unlock diverse object and environmental interactions.

II. A ROPE-BASED MANIPULATOR

A. Manipulator design

The rope-based manipulator was designed to: i) accelerate a chosen rope to a sufficient ToV such that it enters the air-lifted state; ii) control the loop shape so it can interact with various objects and retract those objects inwards to a secured storage position; and iii) utilize wireless communication and an integrated power supply such that it can be equipped as a standalone module to a robot's end-effector. Fig. 2b illustrates the prototype and labels the various components that address the aforementioned functionalities. The manipulator consists of two brushless direct current motors (AS23173, T-MOTOR; they have a maximum speed of 15000 RPM) (1) that each rotate a rubber wheel (2). The wheels impart force on the rope as it moves through the system. Each having a radius of 15 mm, the wheels are made of 3D printed polylactic acid with a layer of rubber on the outside to increase the friction. After being ejected through the opening after the wheels, the rope returns back to the wheels via a rope guide, which is an eyelet (3). A servo motor (Dynamixel AX-12a, Robotis) (4) rotates a spindle (5) to move the rope guide along a linear trajectory. As such, the loop diameter can be adjusted in real time for tightening around an object or grasping differently-sized objects.

All of the electronics for power and control of the actuators reside onboard the prototype. Control of all subsystems is accomplished via a microcontroller (MKR WiFi 1010, Arduino) (6), which we chose because of its small form factor and built-in WiFi module for wireless control. Directly attached to the Arduino is a motor controller (Dynamixel Shield, Robotis) that interfaces with the motors that drive the spindle. To control the motors driving the wheels, we used two electronic speed controllers (Tekko32-F3 65A, HEBU-Shop). Power for all the electronics is provided by two batteries: a 12V LiPo battery (7) to power all the motors and a 3.7V Li-Ion battery (8) to power the microcontroller. These batteries support a runtime of approximately 15 minutes. Finally, there is a rotary magnetic encoder (RMD08D0115, RML) (9) on one of the BLDC motors that measures the RPM to control the rope velocity.

The velocity required to make the rope float is proportional to its linear mass, μ. We used a braided natural wool rope ($\mu = 0.221$ g/m), which by interpolating from experiments performed in reference [12], has a ToV of 2.6 m/s. The ends of the rope are connected together with general purpose glue and can withstand a tensile force of approximately 10 N before separation. Fixing the type and length of the rope, the parameters that can influence the loop shape are reduced to the rope velocity, v_{rope}, and the ejection angle of the rope, ϕ [12]. Both of these parameters can be controlled by the manipulator system during operation.

B. Manipulator characterization

To obtain a qualitative understanding of interacting with objects with the rope-based manipulator, we manually performed grasping experiments on a selection of objects in-

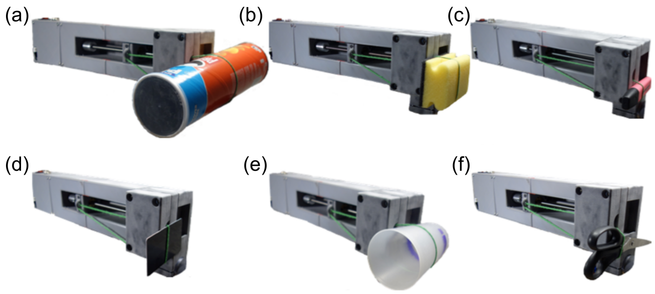

Fig. 3. Manipulator having wrangled and retracted diverse objects to a stowed position: (a) chips can, (b) sponge, (c) marker, (d) credit card, (e) cup, (f) scissors. Many objects are graspable due to the compliance of the rope.

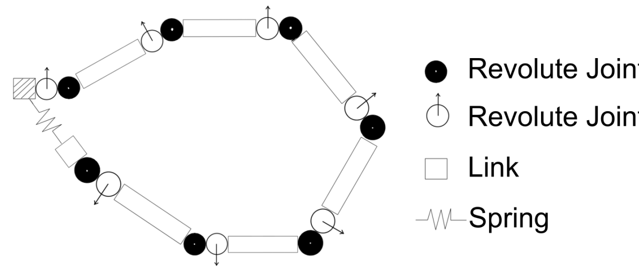

Fig. 4. Schematic of the kinematic chain model used in the simulation of the rope manipulator. Black filled revolute joint has in-plane axis. White filled revolute joint has out-of-plane axis.

Class	Object	Graspable
Food	Chips Can	✓
	Tuna Fish Can	✓
	Banana	✓
	Apple	
	Orange	
Kitchen Items	Sponge	✓
	Spoon	✓
	Fork	✓
	Mug	✓
Tools	Scissors	✓
	Permanent Marker	✓
	Phillips Screwdriver	✓
Misc. Items	Credit Card Blank	✓
	Cups	✓
	Tennis Ball	
	Golf Ball	

TABLE I
GRASPING SUCCESS OF THE MANIPULATOR FOR VARIOUS OBJECTS FROM DIFFERENT OBJECT CLASSES.

spired by the YCB Object and Model Set [17], [18], [19]. First, we activated the manipulator to form a stable loop. Then, we moved the loop around the object of interest, which was at rest on a flat surface. Next, we allowed the loop to relax and conform to the object it was placed around. Finally, we actuated the retraction DoF to reel in and secure the object against the manipulator.

We found that the manipulator can successfully grasp, reel in, and secure cylindrical and box-like geometries. Spherical geometries (e.g. sports balls) pose difficulties because the rope tends to slip off the convex surface and no stable regions for the rope to wrap around are present (Fig. 3; Tab. I). In all cases, the actively moving rope deflects when it touches an object, and exhibits oscillations originating about the contact line with the object. We observed that the line of contact between the rope and the object is narrow. Therefore, successful grasps require the location of this line to be close to the center of mass of the object or else there is a risk that the object rotates and falls out of the loop as the retraction DoF is moving it into the secured position on the manipulator.

The manipulator was also verified to operate with ropes ranging from 40 cm to 200 cm in length. While the manipulator retraction DoF stroke length is limited to 18 cm, simply changing the length of the rope adjusts the size class of objects that can be interacted with and thus serves to adapt the manipulator to the constraints of the environment. By varying the length of the rope, we successfully wrangled objects ranging from 2 cm to 80 cm in length. Our choice of rope limited our experiments to object weighing up to 1 kg, though higher tensile strength and an improved end-to-end connection by melting the ends together can substantially increase the maximum weight capacity of the manipulator. These preliminary observations and experiments of the rope-based manipulator compelled us to devise a physical model to further understand its behavior and also provide a launching point for future wrangling controllers.

III. Modeling and Simulation

A. Discretized rope manipulator model

The previous qualitative characterization experiments revealed that the rope manipulator in its free-floating state exhibits a duality of regimes: i) nominal quasi-static loop shape when not contacting an object, and ii) deforming of the loop upon contacting an object, characterized by oscillations that eventually transition to a stable state again after the contact condition is removed. To recapitulate the manipulator's interaction mechanics in both regimes, we opted to create a new model that could account for contacts (previous models for string-shooters, such as those proposed in refs. [12], [13], do not consider contacts).

We assume that the behavior of the rope around steady state rotation speed (at or exceeding ToV) can be modeled as a kinematic chain consisting of N links, where each link includes two revolute joints on each of its sides. One joint rotates in the plane formed by the opening of the rope, and the other rotates laterally out of this plane (note: in-plane refers to the plane of the drawing in Fig. 4). We implemented this model in IsaacGym, where the joints were controlled with PD controllers. The loop was closed by applying an artificial spring force from the last link of the chain to the base link. See `https://github.com/leggedrobotics/robowrangler` for the code.

Our modeling approach deviates from a discretized rope whip model proposed by Nah et al. [20], which uses spherical joints. Instead, we use two revolute joints so that we

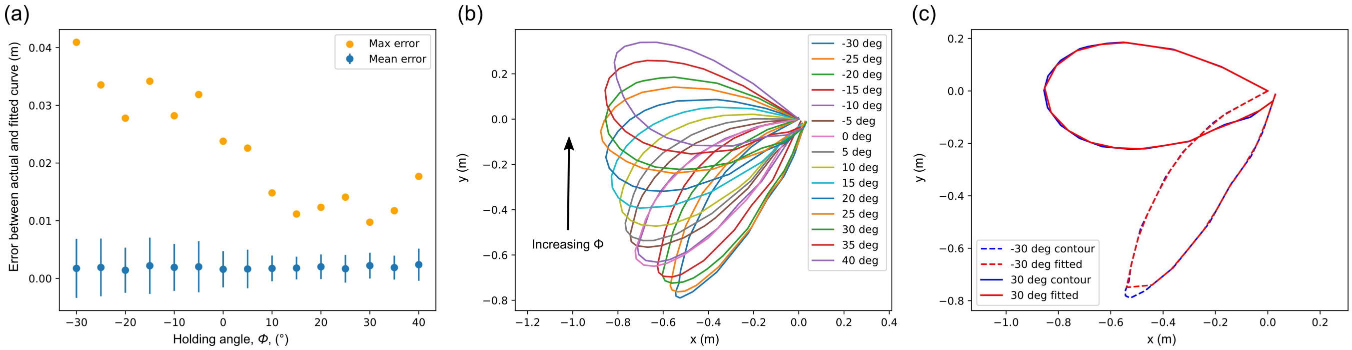

Fig. 5. (a) Maximal and mean discretization errors between the experiment and fitted loop shapes with 20 segments, across different inclination angles, ϕ, and using a 2m-long rope loop. Mean points are calculated over five trials and include the standard deviation as error bars. (b) Example fitted rope shapes at different ϕ. Note: this diagram assumes the rope is being accelerated from right to left, and gravity acts downward along the y-axis. (c) Comparison of the experimentally extracted contour and the fitted model curve for the cases of ϕ =-30 and 30°.

can specify the mechanical properties of each deformation axis separately. This is necessary because we empirically observed that the loop is stiffer in-plane than out-of-plane, and that the top branch of the loop is stiffer than the bottom branch. As such, the in-plane joints of the upper branch of the rope have finite stiffness while the in-plane joints of the lower branch have zero stiffness. All out-of-plane joints have zero stiffness. All in-plane joints have proportional gains of 10000 and damping coefficients of 5000. These gain values ensure fast convergence to the steady state shape upon a change of angle applied to the rope base, mirroring the behavior of the physical system and preventing simulation instabilities.

The loop shape varies with respect to its orientation in the gravitational field. Therefore, we opted to empirically identify its shape at different values of inclination, ϕ, and to interpolate the shape with respect to this parameter for use in the simulated model. The interpolated shape serves to adjust the lengths and angles in the kinematic chain to achieve the desired shape in simulation.

To characterize the rope loop shape at different inclination angles with respect to gravity, the manipulator was fixed at 5° increments ranging from $\phi = -30°$ to $40°$. Pictures were taken at every configuration. These images were cropped and binarized. Next, the rope contour was extracted with the algorithm proposed in [21] (prebuilt natively in OpenCV). Then, N roughly equally spaced points from the contour were extracted to form the segment endpoints of the kinematic chain. The x and y coordinates of the N points were then interpolated with cubic splines, mapping the rope angle to points.

While the model in simulation is running, a given ϕ is input and then the angles between subsequent segments are computed and used as target values for the in-plane revolute joints. The target values for the out-of-plane revolute joints remain at zero because the rope returns to its nominal configuration when undisturbed.

B. Evaluation at steady state

We first evaluated the accuracy of the model at different ϕ values. All evaluations were carried out with the same rope used in the rope-based manipulator and at analogous speed regimes, but with a miniature string shooter rather than the full manipulator. The distance between every point in the experimentally determined contour to the model was computed.

The maximal and mean deviations of the points for each ϕ is shown in Fig. 5a. As can be seen, the maximum deviation is greatest at negative values of ϕ. At these angles, the loop assumes an ellipsoid shape with a larger major axis, resulting in a higher value of curvature at the tips. Fig. 5b shows the fitted curves across all tested angles, and the trend toward more elliptic shapes is clearly seen. The higher curvature of the tips of the ellipsoid causes the linear discretization to be less accurate. Fig. 5c depicts the particular case where ϕ =-30°, where this phenomenon is quite evident. Despite boundary effects, the maximal deviation over all inclination angles amounts to 4 cm—representing 2% of the entire loop length. These results testify that the discretization model captures the rope shape fairly accurately.

C. Evaluation during dynamic contactless movement

The rope reacts to changes in the manipulator's position and orientation with a short transitory phase in which it settles into a new steady state (See Supplementary Video for examples of all evaluations). At slow movement speeds, this transitory phase appears to be well-approximated using a classical spring damper system, and so it is accurately captured by our model (Fig. 6a). At higher movement speeds, especially with sudden changes in the direction of movement, the transitory phase becomes more complex and cannot be accurately approximated by our model.

D. Evaluation during contact

Some contact conditions deform the the steady state of the rope but do not induce high amplitude destabilizing oscillations. For example, in the case of contacting a door handle (Fig. 6b) or wrapping around a cylindrical object (Fig. 6c), our simulation matches the real behavior closely. For instance, in the latter case, the lower branch of the loop deforms around the pole, while the upper branch remains undeformed. Contact conditions with the upper branch proved to be comparatively difficult to capture with the model. For

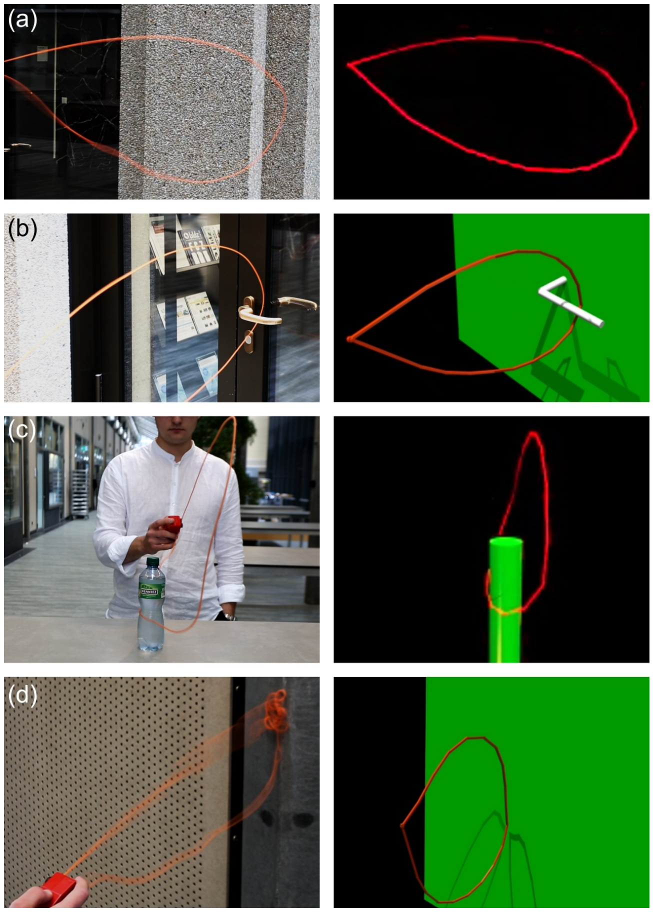

Fig. 6. Juxtaposition of real rope shapes (using a toy string shooter as a baseline with a 40 cm-long rope) with simulation model implemented in IsaacGym environments. (a) Steady-state movement with no contact. (b) Wrapping around a door handle. (c) Wrangling a cylindrically-shaped object. (d) Pressing against a flat surface.

example, when directly pressed against a flat surface (Fig. 6d), the rope undergoes chaotic entangling and de-tangling that cannot be accurately portrayed by the kinematic chain model.

IV. Integration with a quadrupedal robot

A. Setup

We equipped the manipulator to a quadrupedal robot (ANYmal D, ANYbotics) and assessed its potential to expand the robot's capacity to pick up various objects and interact with infrastructural features in its environment (Fig. 7). To enable the positioning of the manipulator in relation to the object, the quadruped was deployed with a reinforcement learning-based controller that facilitates balancing with only three of its legs while the fourth leg is used for manipulation [22]. The fourth leg was outfitted with the manipulator. Both the robot's pose and the activation of the manipulator were manually teleoperated.

B. Wrangling results

The rope-based manipulator allowed the robot to grasp several common objects in human environments across a range of sizes, masses, and textures (See Supplementary Video). For instance, the robot was able to walk up to a tool set and grasp a screw driver (Fig. 7a). As an added benefit, the robot was able to use the manipulator to pull in the screwdriver and then walk away with the screwdriver secured against the shank. In addition, the robot was able to open doors by looping the rope around the handle and then pulling backward (Fig. 7b). Lastly, the robot was able to wrangle and engage in manipulation of a trash can with radius of 50 cm. (Fig. 7c)

Throughout tests, we found that precise alignment of the robot's end-effector with objects and features of interest was not necessary due the fact that rope passively conformed to the geometry of whatever it interacted with—reinforcing the benefits of the physical intelligence afforded by rope. Overall, using one of the robot's existing legs as a manipulation device seems to have yielded certain advantages over installing an articulated manipulator atop the base—as has been historically the paradigm [23] and is still today common practice [24]—in terms of weight, agility, power consumption, and reachable workspace.

V. Conclusion and Future Work

To summarize, we developed a rope-based manipulator that renders a free-floating loop shape whose size can be adjusted on demand, and began to investigate its potential for object manipulation and environmental interaction. We found that rope-based manipulation can effectively handle objects of varying shapes, textures, and sizes. While the current prototype demonstrated limitations in terms of handling spherical objects and has restrictions on the maximum tensile force it can sustain, future improvements in adhesion techniques and rope selection could address these issues.

We also introduced an identification pipeline for a contact-aware rope model and implemented the model as a simulation module for IsaacGym. The model sheds light on regimes of the rope-manipulator during contact and non-contact conditions. Furthermore, it provides a starting point for exploring controllers derived in a simulated environment. While the model accurately captures quasi-static behavior, its limitation is replicating high-frequency, chaotic contact dynamics, fast movements of the rope, and the out-of-plane dynamics.

Looking ahead, the concept of rope manipulation offers exciting possibilities. Multiple ropes with different properties could be coordinated to ensnare and retract objects. A rope manipulator could also one day let robots perform self-manipulation (e.g. facilitating climbing vertical surfaces), enhancing their maneuverability in complex spaces. By integrating rope-based manipulation into robotic systems, we can pave the way for more sophisticated and adaptable robots that seamlessly interact with the human world.

VI. Acknowledgments

We would like to thank Philip Arm and Dylan Vogel for their assistance with robot demonstrations. This work was

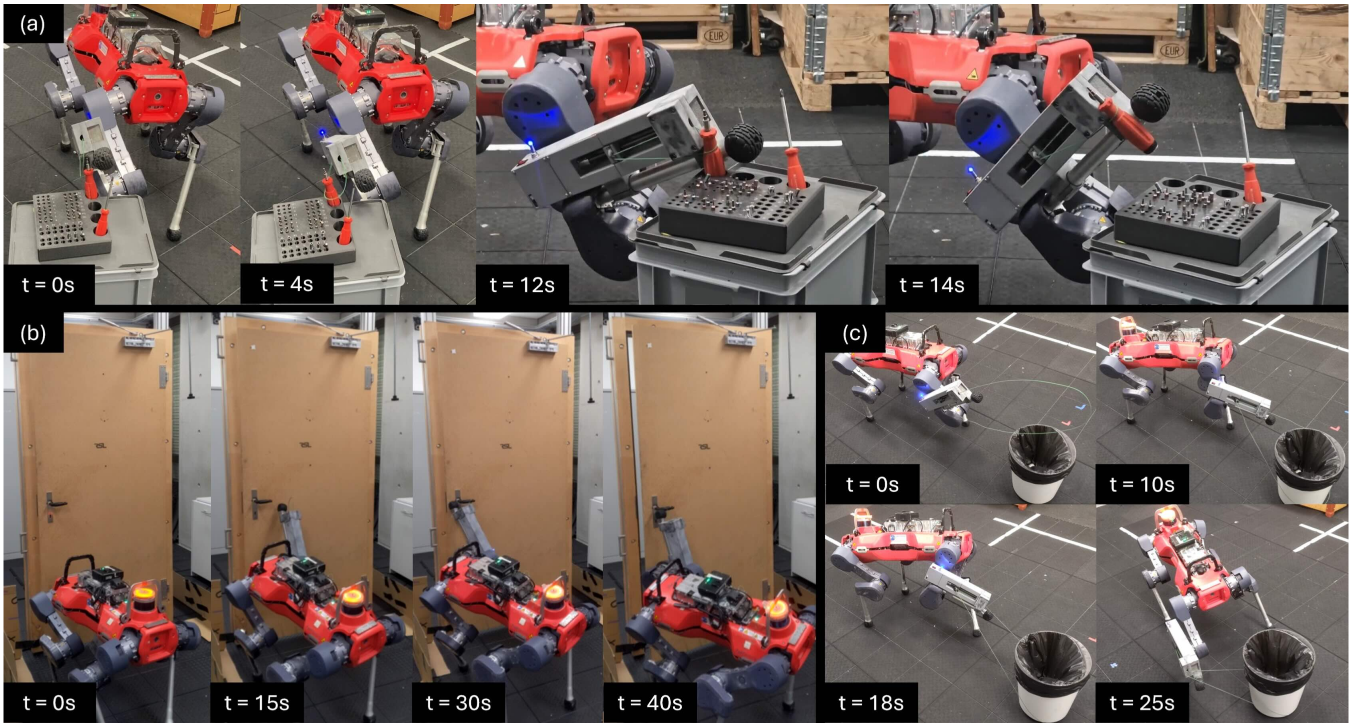

Fig. 7. When equipped to the end-effector of a quadruped robot, the manipulator expands the functional interaction capabilities of the robot to different objects and infrastructural features in its environment. For instance, the manipulator enables the robot to: (a) pick up a screwdriver, (b) open a door, and (c) wrangle and move a trashcan.

supported by The Branco Weiss Fellowship - Society in Science, administered by ETH Zurich.

References

[1] A. Billard and D. Kragic, "Trends and challenges in robot manipulation," *Science*, vol. 364, no. 6446, p. eaat8414, 2019.

[2] I. D. Walker, "Continuum Backbone "Continuum" Robot Manipulators," *International Scholarly Research Notices*, 2013.

[3] C. Melchiorri and M. Kaneko, *Robot Hands*. Cham: Springer International Publishing, 2016, pp. 463–480.

[4] J. Butterfass, M. Grebenstein, H. Liu, and G. Hirzinger, "Dlr-hand ii: next generation of a dextrous robot hand," in *Proceedings 2001 ICRA. IEEE International Conference on Robotics and Automation (Cat. No.01CH37164)*, vol. 1, 2001, pp. 109–114 vol.1.

[5] M. E. Giannaccini, I. Georgilas, I. Horsfield, B. H. Peiris, A. Lenz, A. G. Pipe, and S. Dogramadzi, "A variable compliance, soft gripper," *Autonomous Robots*, vol. 36, no. 1-2, p. 93–107, Jan 2014.

[6] S. Hirose and Y. Umetani, "The development of soft gripper for the versatile robot hand," *Mechanism and Machine Theory*, vol. 13, no. 3, pp. 351–359, 1978.

[7] K. Becker, C. Teeple, N. Charles, Y. Jung, D. Baum, J. C. Weaver, L. Mahadevan, and R. Wood, "Active entanglement enables stochastic, topological grasping," *Proceedings of the National Academy of Sciences*, vol. 119, no. 42, p. e2209819119, Oct. 2022.

[8] H. A. McKenna, J. W. S. Hearle, and N. O'Hear, *Handbook of fibre rope technology*. Woodhead publishing, 2004, vol. 34.

[9] A. Nair, D. Chen, P. Agrawal, P. Isola, P. Abbeel, J. Malik, and S. Levine, "Combining self-supervised learning and imitation for vision-based rope manipulation," 2017.

[10] P. Sundaresan, J. Grannen, B. Thananjeyan, A. Balakrishna, M. Laskey, K. Stone, J. E. Gonzalez, and K. Goldberg, "Learning rope manipulation policies using dense object descriptors trained on synthetic depth data," in *2020 IEEE International Conference on Robotics and Automation (ICRA)*, 2020, pp. 9411–9418.

[11] P.-T. Brun, N. Ribe, and B. Audoly, "An introduction to the mechanics of the lasso," *Proceedings of the Royal Society A: Mathematical, Physical and Engineering Sciences*, vol. 470, no. 2171, p. 20140512, 2014.

[12] Abello, Margaux, Courson, Juliette, Maury, Arnaud, and Renaud, Julian, "String shooter´s overall shape in ambient air," *Emergent Scientist*, vol. 4, p. 1, 2020.

[13] N. Taberlet, J. Ferrand, and N. Plihon, "Propelled strings: Rising from friction," *Phys. Rev. Lett.*, vol. 123, p. 144501, Oct 2019.

[14] A. Daerr, J. Courson, M. Abello, W. Toutain, and B. Andreotti, "The charmed string: self-supporting loops through air drag," *Journal of Fluid Mechanics*, vol. 877, p. R2, 2019.

[15] K. Mamola, "Physics of the String Shooter," *The Physics Teacher*, vol. 61, no. 5, pp. 328–330, 05 2023.

[16] M. Sitti, "Physical intelligence as a new paradigm," *Extreme Mechanics Letters*, vol. 46, p. 101340, 2021.

[17] B. Calli, A. Walsman, A. Singh, S. Srinivasa, P. Abbeel, and A. M. Dollar, "Benchmarking in manipulation research: Using the yale-cmu-berkeley object and model set," *IEEE Robotics and Automation Magazine*, vol. 22, no. 3, pp. 36–52, 2015.

[18] B. Calli, A. Singh, J. Bruce, A. Walsman, K. Konolige, S. Srinivasa, P. Abbeel, and A. M. Dollar, "Yale-cmu-berkeley dataset for robotic manipulation research," *The International Journal of Robotics Research*, vol. 36, no. 3, pp. 261–268, 2017.

[19] B. Calli, A. Singh, A. Walsman, S. Srinivasa, P. Abbeel, and A. M. Dollar, "The ycb object and model set: Towards common benchmarks for manipulation research," in *2015 International Conference on Advanced Robotics (ICAR)*, 2015, pp. 510–517.

[20] M. C. Nah, A. Krotov, M. Russo, D. Sternad, and N. Hogan, "Manipulating a whip in 3d via dynamic primitives," in *2021 IEEE/RSJ International Conference on Intelligent Robots and Systems (IROS)*. IEEE, 2021, pp. 2803–2808.

[21] S. Suzuki, "Topological structural analysis of digitized binary images by border following," pp. 32–46, 1985.

[22] P. Arm, M. Mittal, H. Kolvenbach, and M. Hutter, "Pedipulate: Enabling manipulation skills using a quadruped robot's leg," 2024.

[23] O. Khatib, "Mobile manipulation: The robotic assistant," *Robotics and Autonomous Systems*, vol. 26, no. 2-3, pp. 175–183, Feb. 1999.

[24] J.-P. Sleiman, F. Farshidian, and M. Hutter, "Versatile multicontact planning and control for legged loco-manipulation," *Science Robotics*, vol. 8, no. 81, p. eadg5014, Aug. 2023.